Unusual Crystallization Kinetics in a Hard Sphere Colloid-Polymer Mixture

Thomas Palberg and Andreas Stipp
Johannes Gutenberg Universität, Institut für Physik, Staudingerweg 7, D-55128 Mainz, Germany

Eckhard Bartsch
Albert-Ludwig Universität, Institut für Physikalische Chemie, Albertstrasse 21, D-79104 Freiburg, Germany
(Received 31 January 2008; published 21 January 2009)

We investigated the crystallization kinetics of a hard sphere colloid-polymer mixture at conditions where about 95% of solid coexists with about 5% of fluid. From time resolved Bragg and small angle light scattering, we find that the crystallite size increases with a power law of exponent $\alpha \approx 1/3$ during both the conversion and the coarsening stage. This observation points to a single conserved order parameter for both stages and cannot be explained if the mixture is regarded as an effective one-component system. We alternatively suggest that—based on local geometric demixing—the polymer density takes the role of the conserved order parameter.

DOI: 10.1103/PhysRevLett.102.038302 PACS numbers: 82.70.Dd, 64.70.pv, 81.10.Aj

Colloids in general offer a unique opportunity to precisely tailor particle interactions with experimental means, thus switching from repulsive to attractive, from short to long range from spherically symmetric to dipolar or directed interactions [1]. A direct consequence of this tunability are fascinating options to mimic atomic behavior on a conveniently accessible mesoscopic scale. Charged sphere colloidal crystals, e.g., show metal-like elastic behavior [2], hard sphere (HS) colloids form fragile glasses [3] and oppositely charged particles display a huge variety of salt structures [4,5]. Mixtures of HS and non adsorbing polymers, in particular, serve as weakly attractive model systems [6] conveniently described in effective one-component models [7,8]. Colloid-polymer mixtures (CPM) show a rich phase behavior including crystals, critical and triple point, a reentrant glass transition, and a gel line. Lately, interest shifted to nonequilibrium processes with special focus on phase transition kinetics [1,6,9]. In addition to qualitative observations of kinetic pathways of crystallization [10] and short time studies on spinodal decomposition followed by gravitation induced collapse and/or sediment crystallization [11–13], very recent μg experiments allowed first access to both early and late stages of demixing [14]. In this Letter, we report quantitative crystallization experiments on a density matched HS-CPM at crystal-fluid coexistence over four decades in time covering both the conversion and the coarsening regime. A $t^{1/3}$ growth law of the domain size is observed for both regimes. In addition, Furukawa-scaling [15] is observed for the ringlike small angle scattering pattern occurring for late stage coarsening. Such a behavior is characteristic for phase transitions with stochastic domain growth, absence of hydrodynamics and a conserved order parameter [16–18]. But only for the coarsening stage, a conserved order parameter is expected [19] and in fact has already been reported in the pioneering work of Schätzel and Ackerson [20].

We used surfactant-free emulsion polymerization to synthesize 1:10 crosslinked Polystyrene-microgel particles [21]. Particles were precipitated with methanol and redispersed in Tetrahydrofurane several times to remove monomer, salt, and water. After drying, particles were redispersed in the good solvent 2-ethyl-naphtalene (2EN), where they swell to their maximum size governed by the degree of cross linking: $a = 380 \pm 4$ nm with a polydispersity $\sigma \approx 0.06$ (as determined from static and dynamic light scattering). The corresponding value in the collapsed state was $a_0 = 300$ nm and the swelling ratio $S = a^3/a_0^3 \approx 2.1 \pm 0.1$. Both the density ρ and the refractive index ν are close to the literature values for polystyrene ($\rho_{\mathrm{PS}} = 1.05 g/\mathrm{cm}^{-3}$, $\nu_{\mathrm{PS}} = 1.590$, $\rho_{\mathrm{2EN}} = 0,992\,\mathrm{g/cm}^{-3}$, $\nu = 1.599$ at $T = 293\,\mathrm{K}$). Swollen particles are even better matched, as here the volume weighted quantities apply. Observable sedimentation in our samples occurred only after several weeks.

Unnoticed in earlier work [22], the samples also contain 1.18% w/w of noncrosslinked polymer which could be separated by repeated centrifugation and decantation. The component was dried, weighed, redispersed in THF, and passed through a gel-permeation chromatograph to obtain the molecular weight distribution. We found $M_N = 6.42 \times 10^3$ and $M_W = 1.074 \times 10^4$, which corresponds to a radius of gyration of $r_g \approx 3$ nm in a good solvent. Purified dispersions of microgels in 2EN show typical HS phase behavior, dynamics, and rheology [23,24]. Our contaminated sample was prepared at a nominal volume fraction of $\Phi = 0.54$, i.e., at the upper end of the fluid-crystal coexistence region. The true volume fraction is lower, due to the dissolved polymer: $\Phi_{\mathrm{Part}} = (1 - 0.0118)0.54 = 0.534$. The polymer volume fraction is es-

timated as follows: the particle mass is $m_{\mathrm{Part}} = \rho_{\mathrm{PS}}(4\pi/3)a_0^3 = 1.188 \times 10^{-16}$ kg, the average polymer mass is $m_{\mathrm{Poly}} = M_W/N_A = 1.660 \times 10^{-23}$ kg. This yields a resulting number ratio of $n_{\mathrm{Part}}/n_{\mathrm{Poly}} = (0,9882/m_{\mathrm{Part}})/(0,0118/m_{\mathrm{Poly}}) = 1.2 \times 10^{-5}$. The volume fraction ratio is $\Phi_{\mathrm{Part}}/\Phi_{\mathrm{Poly}} = n_{\mathrm{Part}}V_{\mathrm{Part}}/n_{\mathrm{Poly}}V_{\mathrm{Poly}} = 23.8$. Thus, $\Phi_{\mathrm{Poly}} = \Phi_{\mathrm{Part}}/23.8 = 0.0224$. In turn, this amounts to an effective polymer volume fraction in the solvent of $\Phi_{\mathrm{Poly,eff}} = 0.0481$. With a size ratio of $\chi = a_{\mathrm{Poly}}/a = 0.008$, and the low polymer concentration, we expect no strong deviation from the hard sphere phase behavior [6]. As we shall see, however, the kinetics of crystallization are dramatically different.

Crystallization was studied simultaneously by time resolved Bragg scattering (scattering vectors of 5.2 $\mu\mathrm{m}^{-1} \leq q \leq 19.3\ \mu\mathrm{m}^{-1}$) and small angle light scattering (SALS; $0.028\ \mu\mathrm{m}^{-1} \leq q \leq 0.41\ \mu\mathrm{m}^{-1}$) using a machine already described in detail elsewhere [25]. In short, The sample is placed in an index matching bath with a flat entrance window and a flat outlet for the SALS signal. A widened beam of a He-Ne-laser is focused through the sample onto a beam stop 1.5 m past the sample. A hemispherical lens focuses the Bragg scattered light onto arrays of photodiodes mounted on a rotating arm. A similar construction is used to collect the SALS signal. During measurements, the sample is left at a fixed position, while the detector is rotated about the optical axis. This minimizes mechanical impact on the fragile colloidal crystals, while keeping good statistics. All optical components (bath, cell, lense) are custom made from glass with a refractive index close to that of the sample to avoid reflections and refraction. A time lag of about 1 min separates the cessation of shear (with the sample taken off the tumbler) and the commencement of the first measurement ($t \equiv 0$ with the sample aligned in the machine).

The sample solidified within some 10 minutes after cessation of shear. Microscopy showed that about 95% of the suspension converted into crystalline material, while the remaining melt pockets and grain boundaries took about 5%. From the first five Bragg-peaks, the structure was identified as stacking faulted face centered cubic. All peaks gain intensity and sharpen with time. The {220} reflection was chosen for further evaluation for its strength and unaffectedness by stacking faults. Evaluation followed standard procedures to yield the crystal fraction $X(t)$ from the integrated peak intensity, the crystal volume fraction Φ_X from the peak position and average crystallite dimension $\langle L \rangle_{\mathrm{Bragg}}$ from the full width at half height [26]. Detailed results will be given elsewhere.

Our SALS signals differ from those obtained for pure HS. They occur only after some 200 min and show different scaling relations. Their evolution is shown in Fig. 1(a).

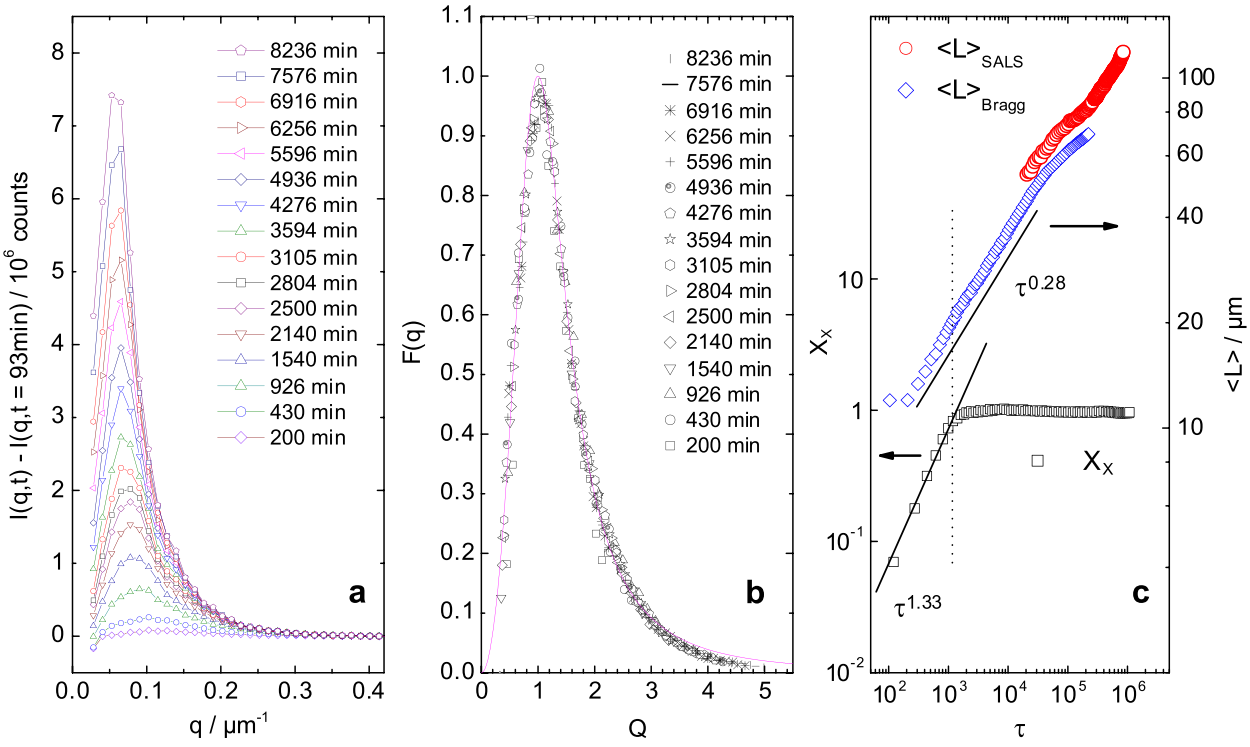

FIG. 1 (color online). (a) Raw SALS data for different times as indicated. (b) Scaled Intensity $F(Q)$ versus scaled scattering vector Q for different times as indicated. The solid line is a fit of Furukawa's function with $d = 2$. Scaling is observed for $t > 200$ min; (c) Double log plots of the temporal evolution (in terms of the reduced time τ) of crystallinity (squares, left scale) and average crystallite size from Bragg scattering (diamonds) and SALS (circles). Lines are power law functions of the indicated exponents and serve as are guides to the eye.

With time, the peak height increases, while the peak position shifts towards lower q. Data collapse on a single curve in Fig. 1(b), if we normalize the intensity to the maximum intensity $I_{MAX}(t)$ and the scattering vector to the position of the maximum $q_{SALS}(t)$. For pure HS, interrupted scaling and long lived transients were observed and attributed to both overlapping depletion zones and an ill-defined transition from the nucleation and growth regime to the ripening regime [25,27–29]. Here, no short time signal from depletion zone scattering is present and we instead obtain continuous late time scaling; i.e., all data follow Furukawa's dynamic scaling function $F(q) = I(q)/I_{MAX} = (1 + \delta/2)Q^2/(\delta/2 + Q^{\delta/2})$, where $Q = q/q_{SALS}$ and δ is related to the dimension d of the scattering objects d as $\delta = d + 1$ [15]. The fit is of remarkably good quality except for $Q > 3$, where the signal to noise ratio is becoming very small. It returns a dimensionality of approximately two. This value is compatible with scattering from crystal facets. Indeed, additional microscopy experiments using differential interference and phase contrast showed that the platelike grain boundaries have a refractive index lower than average and thus may serve as scattering objects. The characteristic SALS dimension $\langle L\rangle_{SALS} = 2\pi/q_{SALS}$ hence corresponds to the distance between opposing facets which for thin grain boundaries approximately equals the average center-center distance of crystallites and thus at $X = 0.95$ is close to the average crystal size.

In Fig. 1(c), we compare these two independent measures for $\langle L\rangle$, to observe near quantitative agreement. Data are plotted versus the reduced time $\tau = t/t_B$ as obtained from scaling the experimental time (in s) with the Brownian time $t_B = a^2/D_0$, where a is the particle radius and $D_0 = 2.22 \times 10^{-13}$ m^2 s^{-1} is the free diffusion coefficient in 2EN. Thus, 1 min corresponds to 102.7 τ. Over the first two decades, $\langle L\rangle_{Bragg}$ increases with a single power law. A least square fit returns an exponent $\alpha = 0.28 \pm 0.015 \approx 1/3$. Later, α drops to $\alpha \approx 0.22$ for an interval of roughly one decade. $\langle L\rangle_{SALS}$ follows this trend exactly, and the ratio $\langle L\rangle_{Bragg}/\langle L\rangle_{SALS} = 0.85 \pm 0.05$ keeps constant for the whole range of overlap. Finally, α returns to its initial value. The lower part of Fig. 1(c) shows the crystal fraction X_X approach its final value of 0.95 also by a power law, this time of exponent $1.33 \pm 0.3 \approx 4/3$ for the first seven minutes. X_X saturates after 10 minutes as indicated by the vertical dotted line. In line with previous studies on HS, the time interval from 7–10 min is identified as the transition from an early conversion stage to a later coarsening stage [3,26–29]. The most striking differences to pure HS at coexistence [20,25–29] are, however, the persistence of the exponent $\alpha = 1/3$ through the transition from conversion to coarsening and the absence of a SALS signal at early times.

First, previously observed early time SALS signals for pure HS were—in combination with a $t^{1/2}$ growth law—attributed to the formation of extended depletion zones about growing crystals [20,28]. The absence of SALS signals at early times, the different growth exponent and an initial crystal volume fraction of $\Phi_x(t = 200\tau) = 0,557$ observed here, indicate the presence of a conversion scenario different to the particle transport controlled conversion in pure HS.

Second, a $t^{1/3}$ growth law corresponding to classical Ostwald ripening has been observed in HS samples close to melting only during coarsening [20,26] but not during conversion. In principle, both exponents may be lowered with increased Φ by polydispersity induced fractionation [30–32]. In fact, recent systematic measurements on fractionating HS (Microgels of polydispersity 0.068) showed a crossover of the exponents at $\Phi = 0.557$–$0,565$ and values of $\alpha \approx 0.1$ [30]. At coexistence, however, all pure HS systems investigated so far showed conversion exponents of 0.5 to 1, clearly differing from the corresponding coarsening exponents of $1/3$ or lower [3,20,25,26,29].

The combination of both observations calls for a single conserved order parameter throughout crystallization. To solve the puzzle, we leave the conventional effective one-component picture (which excellently describes the equilibrium properties of HS polymer mixtures) and explicitly consider our sample as a two component system. When two particles approach to attain their equilibrium position, the polymer component has to leave the region between their surfaces. Any further particle which approaches the formed pair will encounter an increased polymer concentration in the vicinity of the pair. The process repeats and still larger polymer concentrations are obtained about the growing clusters. Given a two phase state at equilibrium, balance of osmotic pressure requires diffusive transport of polymer away from the clusters into the phase depleted of particles. In the present case, we have concentrated crystal and diluted melt or grain-boundary regions. As a strictly local process, the successive addition of particles is independent of the amount of converted material. In addition, it also applies for the coarsening regime, where particles detach from the facet of a given crystal and independently others attach at the opposing surface of a second one. Again, crystallinity is not conserved, but the total polymer concentration is. We therefore suggest that in CPMs with large size difference, the total polymer number density may become the controlling conserved order parameter even at low polymer volume fraction.

How does that compare to the case of liquid gas phase separation observable in CPMs for large volume fractions of larger polymers? First, our system displays small differences in particle density in the coexisting phases, shows good mass density match, and forms a porous solid rather than isolated crystals [33]. For these reasons, gravitational instabilities after conversion (well documented for so many other systems [6,11–13]) are obviously absent, and we directly compare to μg results. Recent studies of spinodal decomposition of CPMs at large polymer content yielded an exponent of $1/3$ at early times, while at later stages,

convective flows along surfaces increased the exponent slowly towards one [14]. The latter behavior is not unexpected by theory [34] and suggests a coupling of the local polymer concentration to the surface tension between gas and liquid phase. In our case, the differences in particle and polymer concentrations between the coexisting melt and crystal are too small to have a dominating influence on the coarsening kinetics.

Rather, we observe a transiently lower value of at intermediate times. A lower exponent at larger times is compatible with the assumption of Lifshitz-Slyosow kinetics, if one allows for the buildup of elastic distortions of the crystal lattice during the continued expansion of crystallites. In fact, in a recent work, Mitchell and Landau showed this in an extensive high precision Monte Carlo simulation of a 2D Ising model with compressibility and variable lattice mismatch. The observed exponent for domain coarsening dropped from $1/3$ in the rigid and in the unstrained compressible case to 0.224 for a lattice mismatch of 4% [35]. The coincidence with the exponent observed here at later times is surely incidental, but in general, that work showed that crystal distortions will decrease the observable exponent. In our case, a substrate field is absent. Strain occurs upon contact between crystallites. After release of strain by further particle rearrangements, the exponent may return to its initial value.

In conclusion, using simple geometrical considerations, we have for the first time demonstrated that in colloidal two component systems, the formation of a densified crystalline particle phase is closely coupled to the diffusive redistribution of the second, nonordering component. Hence, the kinetics of the crystallization process are slaved by the conserved second component density. We anticipate that our findings will strongly stimulate further investigations into many body effects in CPMs. Our study was restricted to the set of parameters, where the effects should be most visible, the upper end of the coexistence region. Further studies going to larger particle volume fraction (where fractionation becomes important), as well as towards lower volume fractions (where crystals, nucleated heterogeneously at the container walls will allow detailed microscopy of flat interfaces) are under way. Finally, there is in fact a four-level hierarchy of order parameters at this particular set of sample parameters: elasticity, total polymer number density, crystallinity, and particle density. This immediately may invoke new general concepts to tailor the solidification process of melts and hence the properties of the resulting solids.

It is a pleasure to thank K. Binder, J. Horbach, W. Paul, T. Schilling for fruitful discussions, I. Weber and T. Eckert for particle synthesis and characterization. Financial support of the DFG (SFB 625, Pa459/8, /12, and /13), the EU MCRT-Network CT-2003-504 712, and the MWFZ, Mainz is gratefully acknowledged.

[1] A. Yethiraj, Soft Matter **3**, 1099 (2007).
[2] D. Reinke *et al.*, Phys. Rev. Lett. **98**, 038301 (2007).
[3] W. van Megen, Transp. Theory Stat. Phys. **24**, 1017 (1995).
[4] E. V. Shevchenko D. V. Talapin, S. O'Brien, C. B. Murray, J. Am. Chem. Soc. **127**, 8741 (2005);
[5] M. E. Leunissen, Nature (London) **437**, 235 (2005).
[6] W. C. K. Poon, J. Phys. Condens. Matter **14**, R859 (2002).
[7] S. Asakura and F. Oosawa, J. Chem. Phys. **22**, 1255 (1954).
[8] A. Vrij, Pure Appl. Chem. **48**, 471 (1976).
[9] V. J. Anderson and H. N. W. Lekkerkerker, Nature (London) **416**, 811 (2002).
[10] W. C. K. Poon *et al.*, Phys. Rev. Lett. **83**, 1239 (1999).
[11] N. A. M. Verhaegh *et al.*, Physica A (Amsterdam) **242**, 104 (1997).
[12] D. G. A. L. Aarts, R. P. A. Dullens, and H. N. W. Lekkerkerker, New J. Phys. **7**, 40 (2005).
[13] E. H. A. de Hoog, W. K. Kegel, A. van Blaaderen, and H. N. W. Lekkerkerker, Phys. Rev. E **64**, 021407 (2001).
[14] A. E. Bailey *et al.*, Phys. Rev. Lett. **99**, 205701 (2007).
[15] H. Furukawa, Adv. Phys. **34**, 703 (1985).
[16] I. M. Liwshitz and V. V. Slyosov, J. Phys. Chem. Solids **19**, 35 (1961).
[17] J. D. Gunton, M. S. Miguel, and P. S. Sahni, in *Phase Transitions and Critical Phenomena*, edited by C. Domb and J. L. Lebowitz (Academic, New York, 1983), Vol. 8.
[18] A. Bray, Adv. Phys. **43**, 357 (1994).
[19] K. Binder, Rep. Prog. Phys. **50**, 783 (1987).
[20] K. Schätzel and B. J. Ackerson, Phys. Rev. E **48**, 3766 (1993).
[21] S. Kirsch *et al.*, Macromolecules **32**, 4508 (1999).
[22] A. Stipp, Chr. Sinn, T. Palberg, I. Weber, and E. Bartsch, Prog. Colloid Polym. Sci. **115**, 59 (2000).
[23] E. Bartsch, T. Eckert, C. Pies, and H. Sillescu, J. Non-Cryst. Solids **307–310**, 802 (2002).
[24] T. Eckert and E. Bartsch, Proc. Roy. Acad. Sci.: Faraday Disc. **123**, 51 (2003).
[25] A. Heymann, A. Stipp, and K. Schätzel, Il Nouvo Cimento D **16**, 1149 (1994).
[26] J. L. Harland and W. van Megen, Phys. Rev. E **55**, 3054 (1997).
[27] Y. He, B. J. Ackerson, W. van Megen, S. M. Underwood, and K. Schätzel, Phys. Rev. E **54**, 5286 (1996).
[28] B. J. Ackerson and K. Schätzel, Phys. Rev. E **52**, 6448 (1995).
[29] Z. D. Cheng *et al.*, Phys. Rev. Lett. **88**, 015501 (2001).
[30] S. Iacopini, T. Palberg, and H. J. Schöpe, Phys. Rev. E (to be published); H. J. Schöpe (private communication).
[31] S. Martin, G. Bryant, and W. v. Megen, Phys. Rev. E **67**, 061405 (2003).
[32] H. J. Schöpe, G. Bryant, and W. v. Megen, J. Chem. Phys. **127**, 084505 (2007).
[33] Y. He, B. Olivier, and B. J. Ackerson, Langmuir **13**, 1408 (1997).
[34] J. K. G. Dhont, J. Chem. Phys. **105**, 5112 (1996).
[35] S. J. Mitchell and D. P. Landau, Phys. Rev. Lett.. **97**, 025701 (2006).